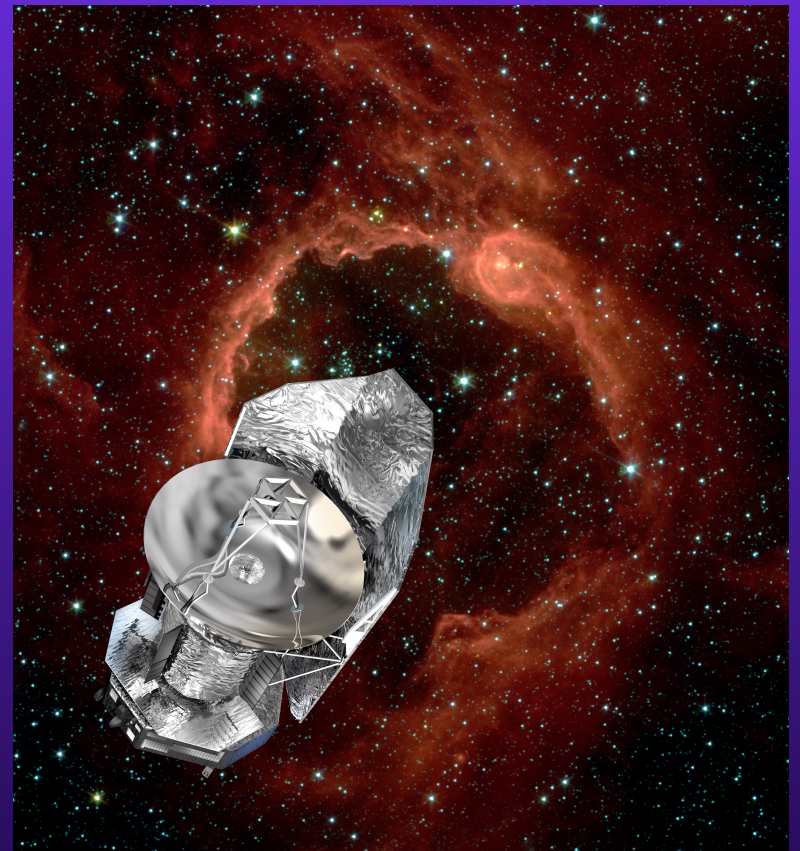


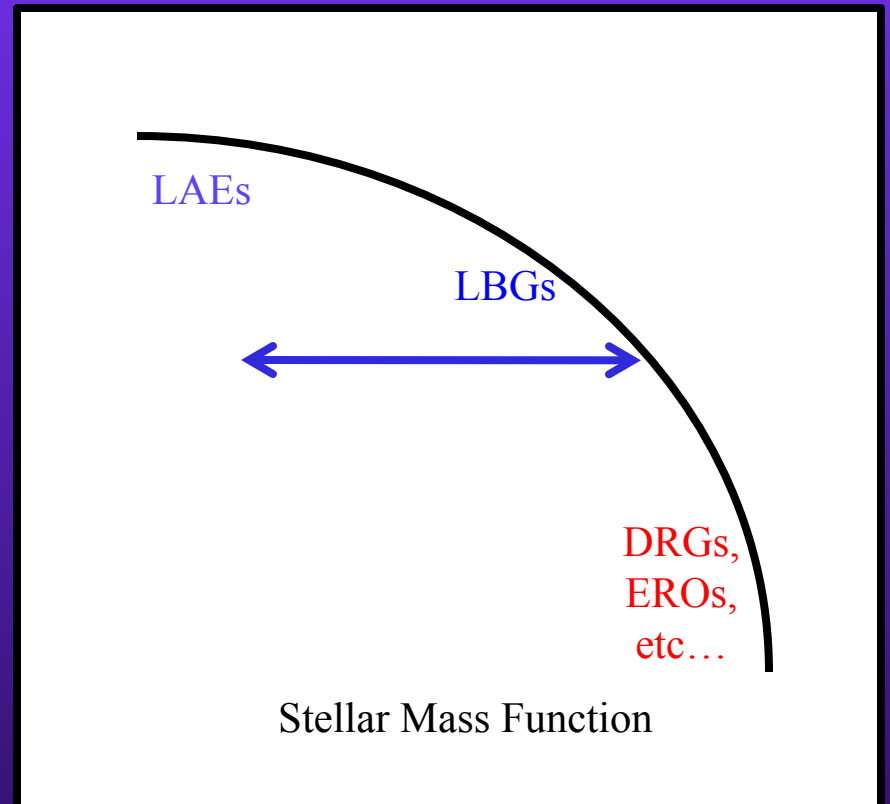
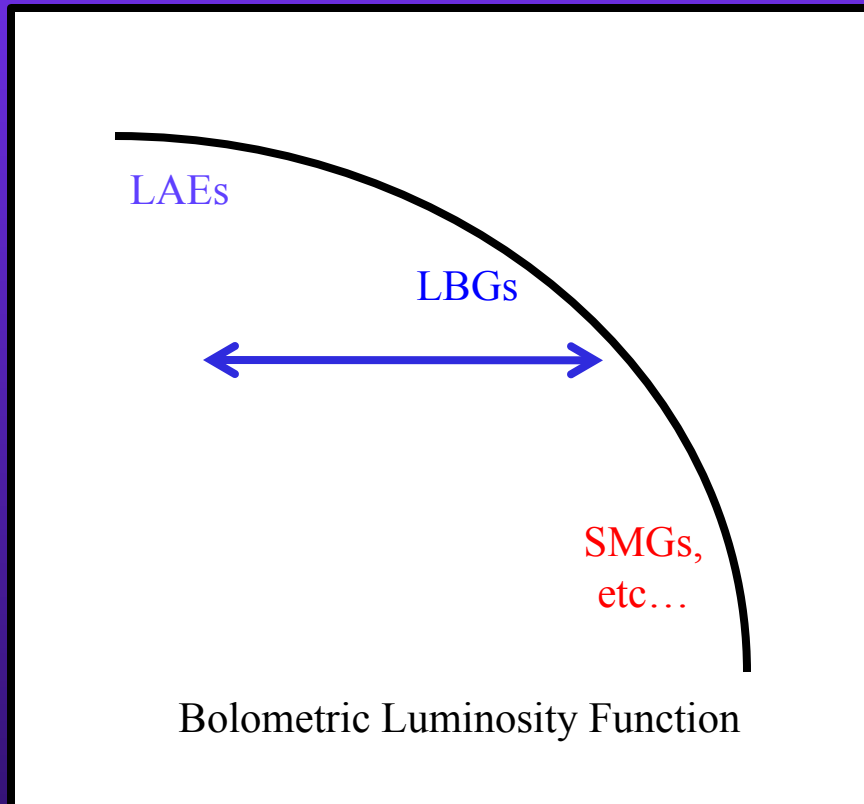
# The Dust Properties of Typical Star-Forming Galaxies at High Redshift

Naveen Reddy (UCR)



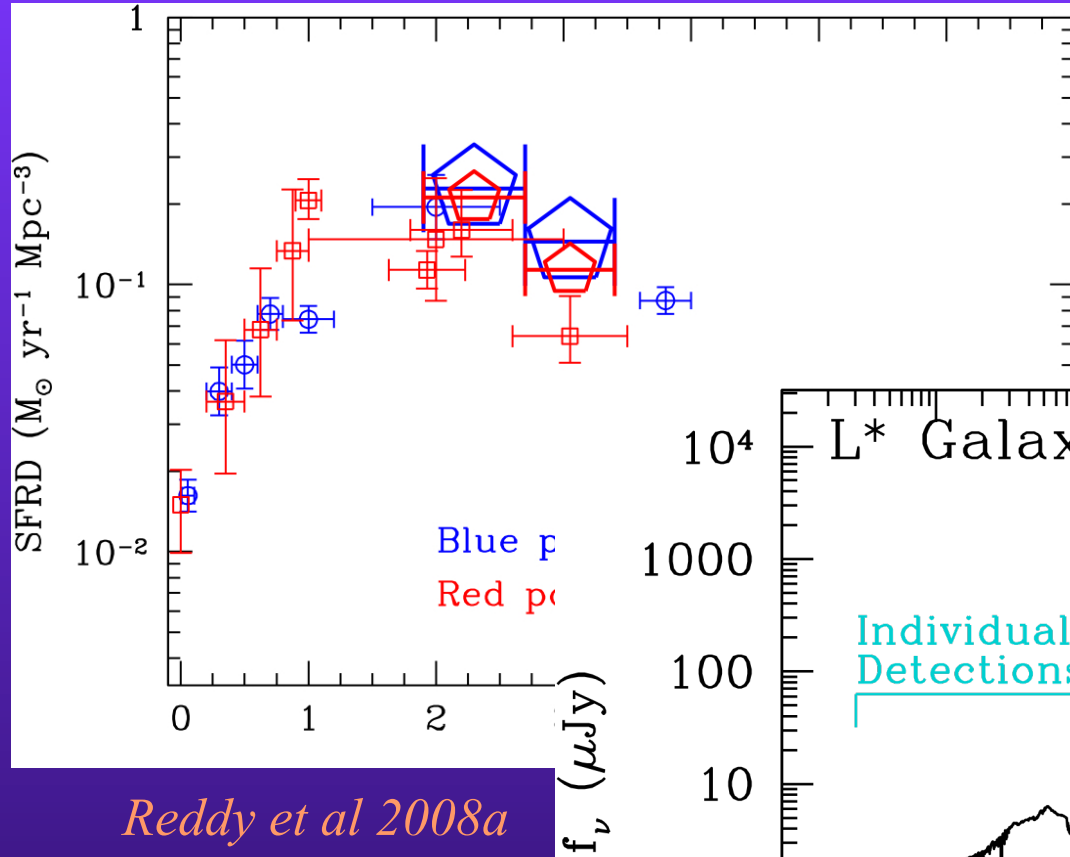
*Through the Infrared Looking Glass, Pasadena, CA, 03 October 2011*

## Some Context: Demographics of $z \sim 2-3$ Galaxies

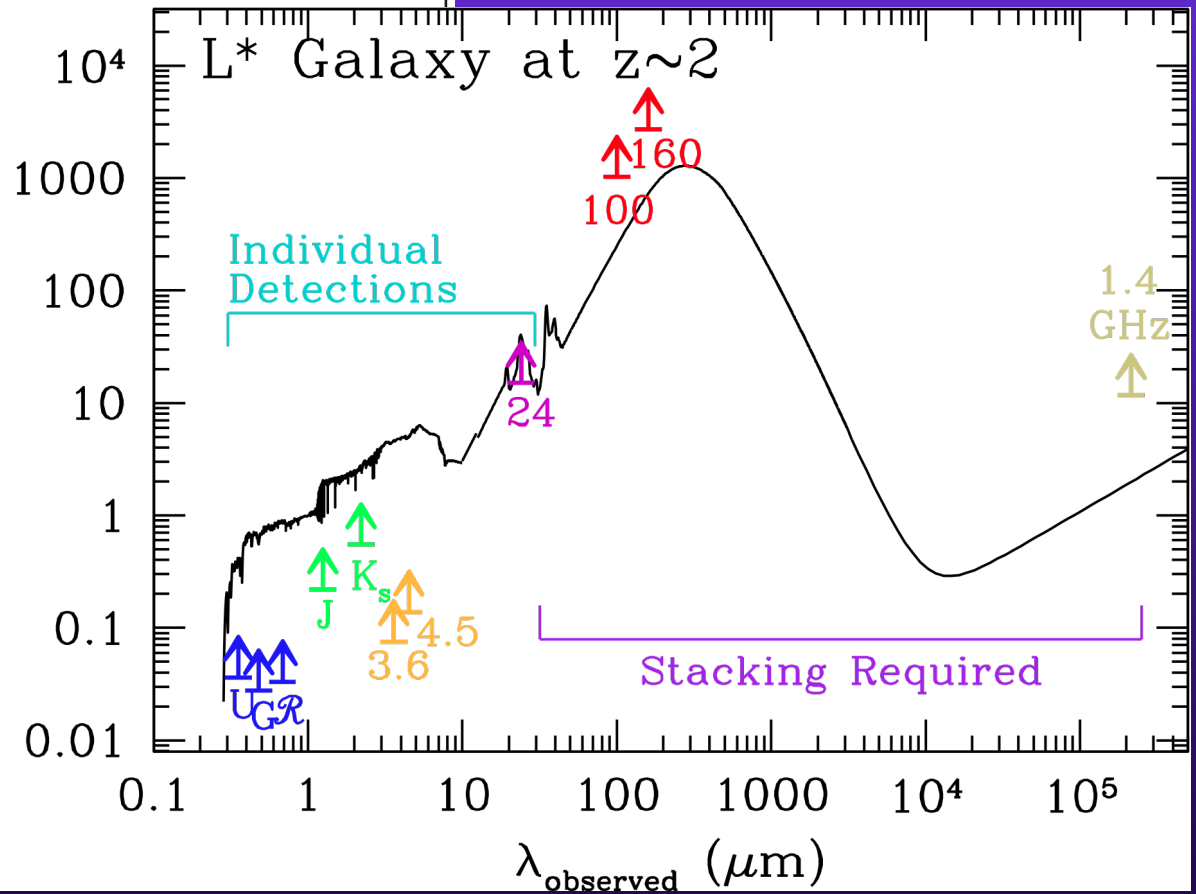


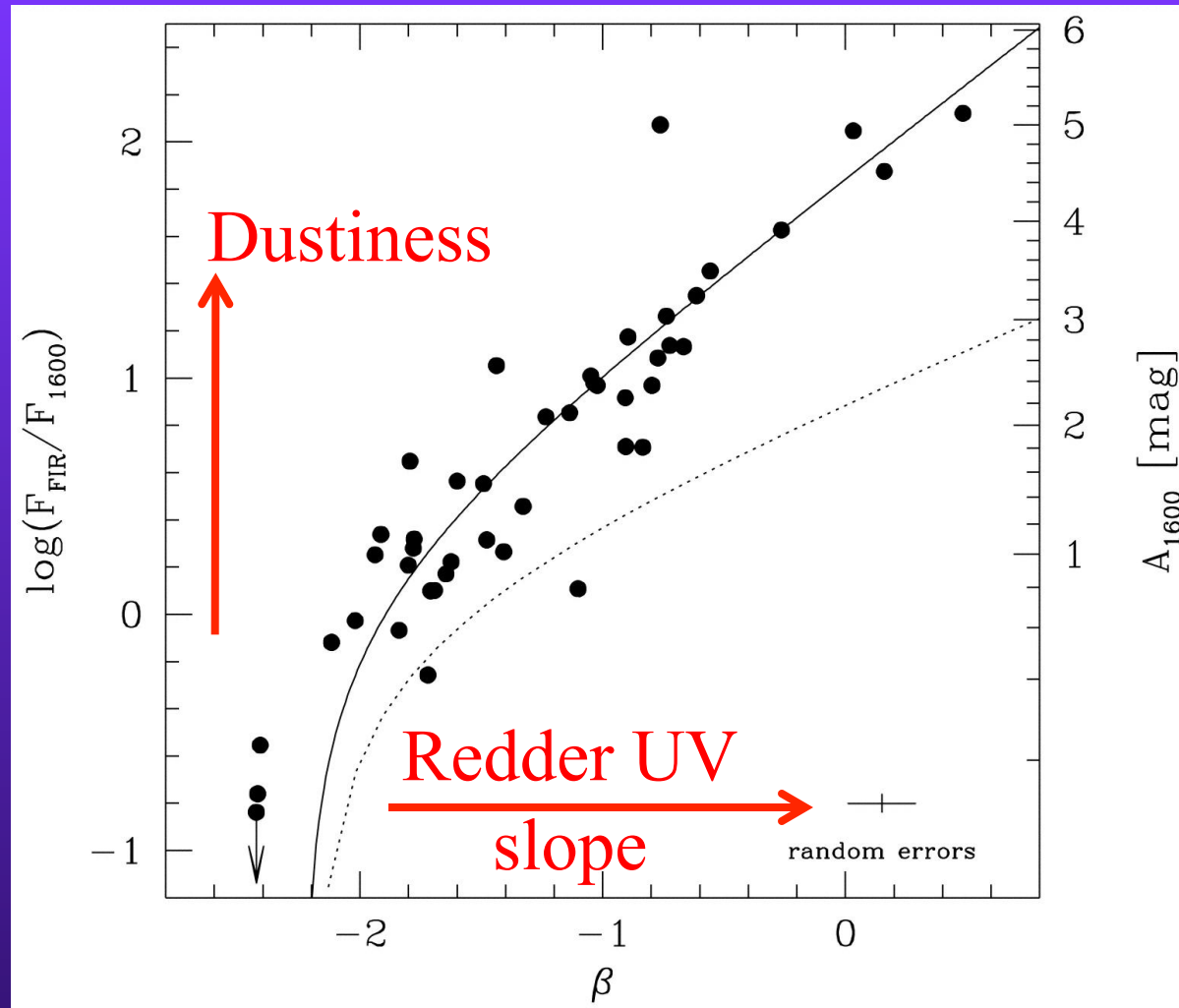
# Motivations

Inferring dust attenuation based on other indicators



*Reddy et al 2008a*





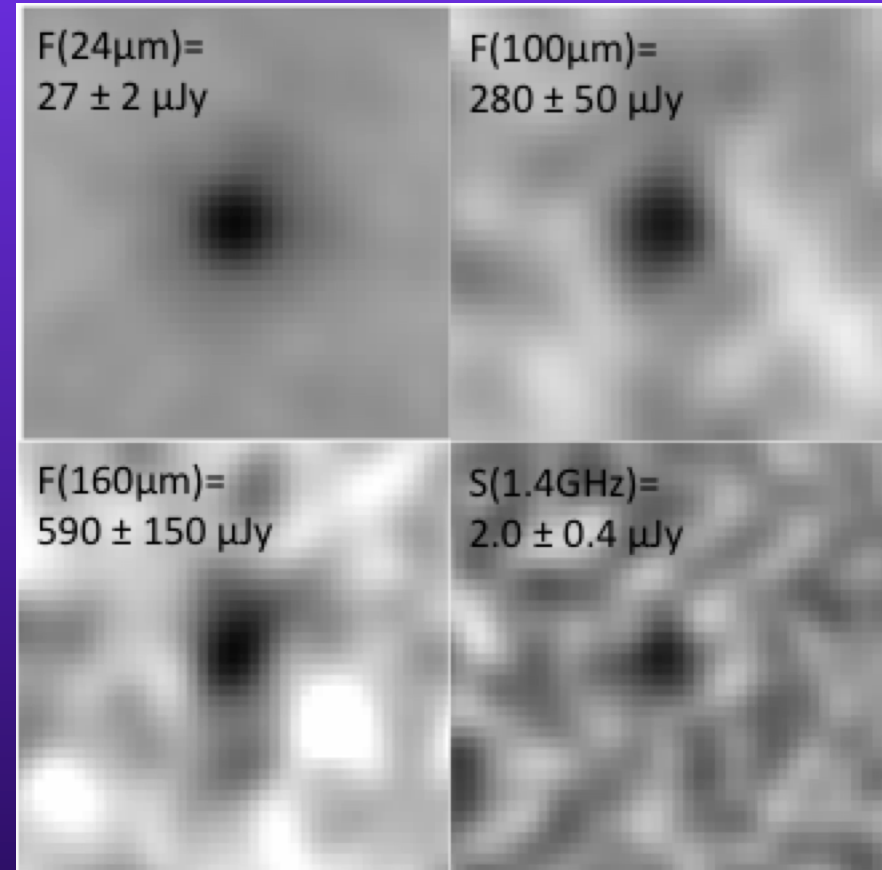
Meurer+99; Calzetti+00





## Herschel Stacking Method

- Stacked spectroscopically confirmed UV-selected galaxies at redshifts  $1.5 < z < 2.6$  in GOODS-North field
- Removed AGN based on presence of optical emission lines and/or power-law SED through the IRAC bands and very high 24 micron flux ( $> \sim 100 \mu\text{Jy}$ )



# Median Dust SED of L\*(UV) galaxy at z~2

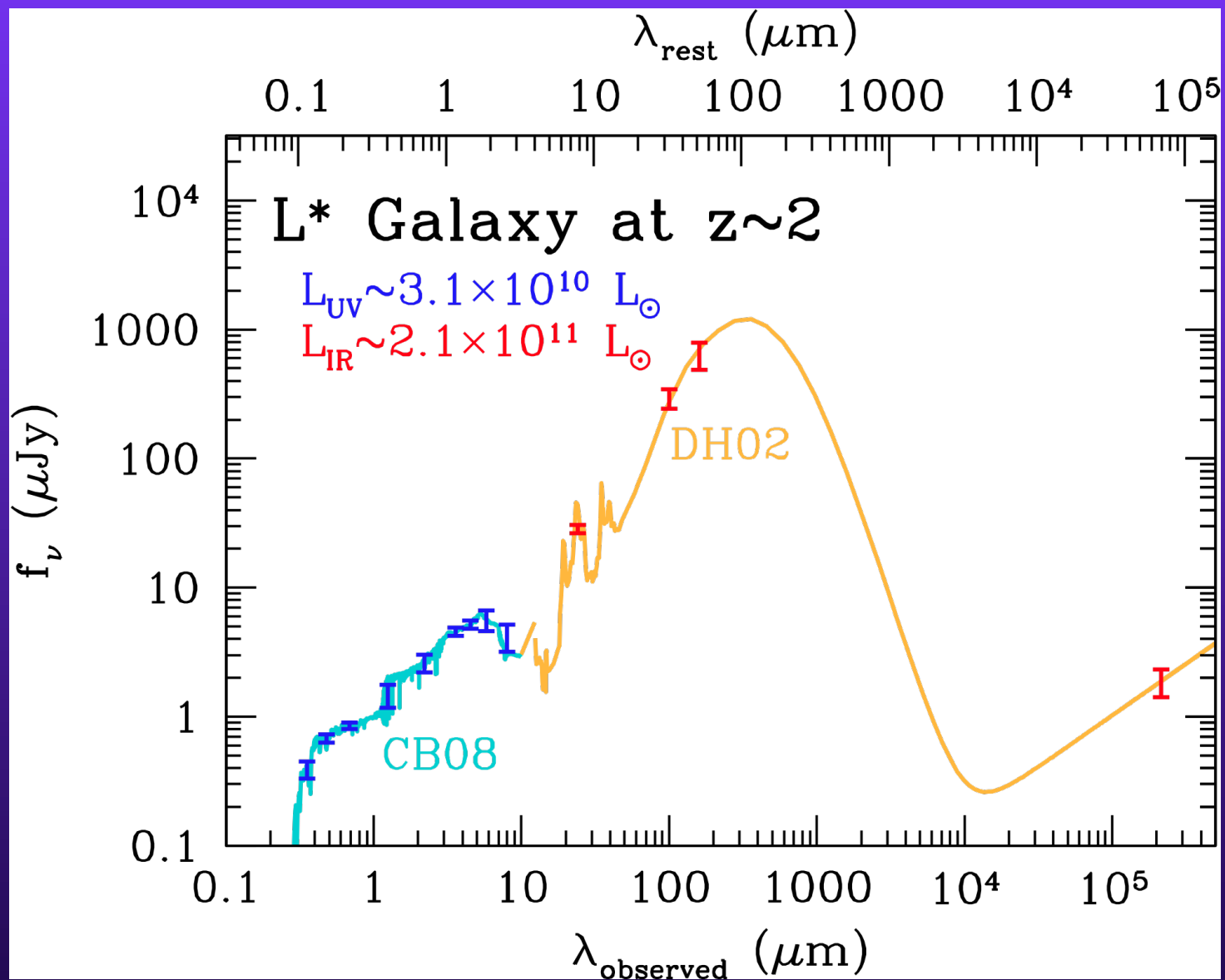


TABLE 1  
COMPARISON OF INFRARED LUMINOSITIES ( $L_{\text{IR}}$ )<sup>a</sup>

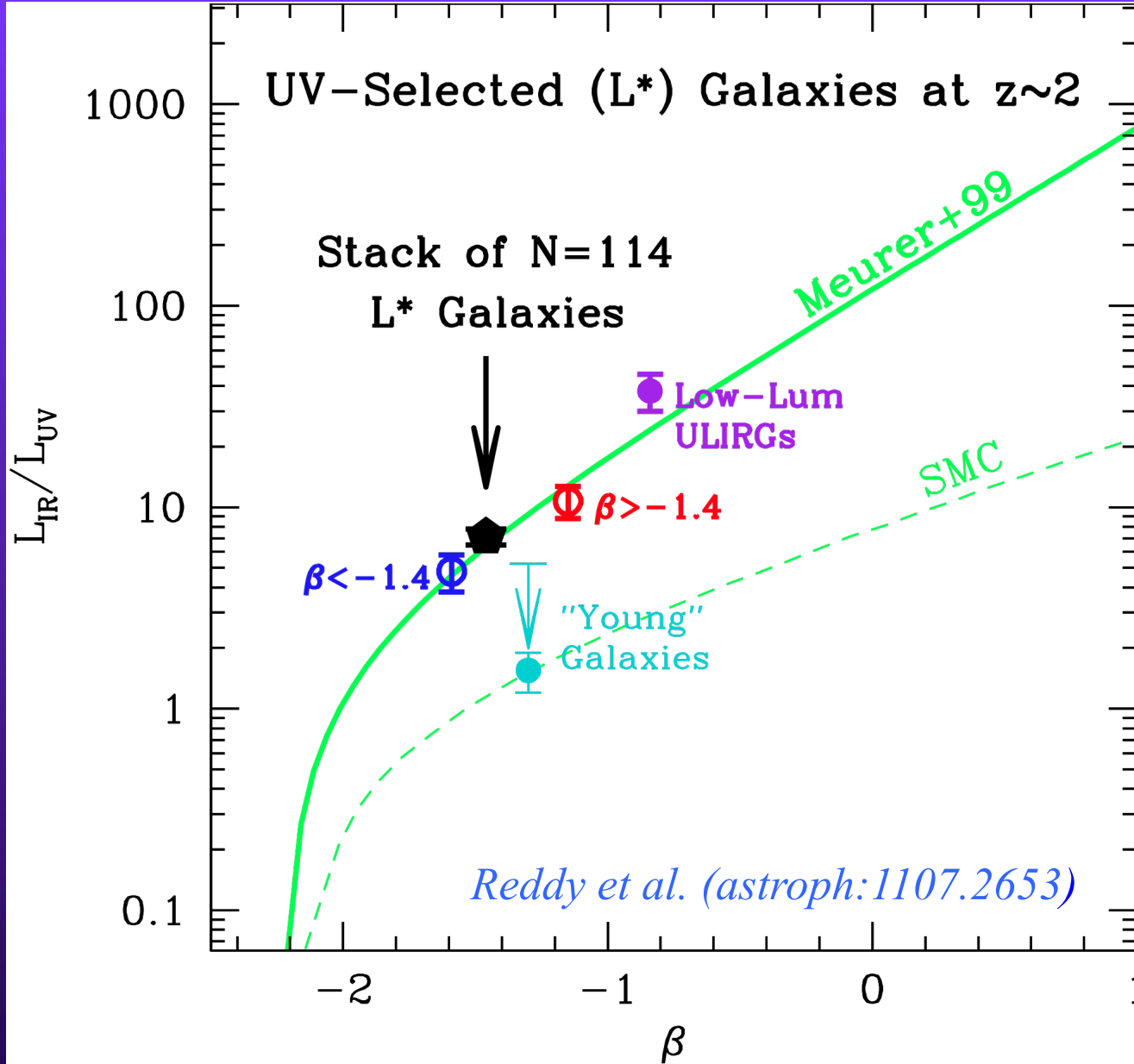
Template	$\lambda, \nu$ <sup>b</sup>	Sample A	Sample B	Sample C	Sample D	Sample E	Sample F
R10a <sup>c</sup>	24	$2.0 \pm 0.3$	$1.8 \pm 0.1$	$1.2 \pm 0.2$	$2.7 \pm 0.2$	$15.7 \pm 0.5$	$0.3 \pm 0.1$
Bell03 <sup>d</sup>	1.4	$2.2 \pm 0.5$	$2.2 \pm 0.4$	$1.7 \pm 0.6$	$2.9 \pm 0.8$	$7.9 \pm 1.7$	$3\sigma: < 3.0$
Elbaz+11-MS Lum <sup>e</sup>	24	$1.9 \pm 0.2$	$1.6 \pm 0.1$	$1.2 \pm 0.1$	$2.2 \pm 0.2$	$9.0 \pm 0.3$	$0.5 \pm 0.1$
...	100	$3.0 \pm 0.4$	$2.9 \pm 0.5$	$2.0 \pm 0.6$	$3.8 \pm 0.7$	$12.7 \pm 1.4$	$3\sigma: < 2.8$
...	160	$3.0 \pm 0.4$	$2.4 \pm 0.6$	$2.1 \pm 0.6$	$2.9 \pm 0.9$	$11.1 \pm 1.7$	$1.7 \pm 1.1$
...	100, 160	$3.0 \pm 0.3$	$2.7 \pm 0.4$	$2.1 \pm 0.4$	$3.5 \pm 0.5$	$12.0 \pm 1.0$	$3\sigma: < 2.8$
...	24, 100, 160	$2.3 \pm 0.3$	$1.7 \pm 0.2$	$1.3 \pm 0.2$	$2.3 \pm 0.3$	$9.2 \pm 0.4$	$3\sigma: < 2.8$
...	24, 100, 160, 1.4	$2.3 \pm 0.3$	$1.7 \pm 0.2$	$1.3 \pm 0.2$	$2.3 \pm 0.3$	$9.2 \pm 0.5$	$3\sigma: < 2.8$
Elbaz+11-MS Lum-Eq Weight <sup>f</sup>	24, 100, 160, 1.4	$3.0 \pm 0.2$	$2.5 \pm 0.2$	$2.1 \pm 0.2$	$3.0 \pm 0.2$	$11.3 \pm 0.3$	$3\sigma: < 2.8$
Elbaz+11-SB Lum <sup>e</sup>	24	$3.7 \pm 0.5$	$3.1 \pm 0.2$	$2.3 \pm 0.3$	$4.3 \pm 0.4$	$17.7 \pm 0.5$	$1.0 \pm 0.2$
...	100	$2.4 \pm 0.3$	$2.3 \pm 0.4$	$1.6 \pm 0.5$	$3.0 \pm 0.5$	$10.0 \pm 1.1$	$3\sigma: < 2.2$
...	160	$2.3 \pm 0.3$	$1.9 \pm 0.5$	$1.7 \pm 0.5$	$2.3 \pm 0.7$	$8.6 \pm 1.3$	$1.3 \pm 0.9$
...	100, 160	$2.4 \pm 0.2$	$2.1 \pm 0.3$	$1.6 \pm 0.3$	$2.7 \pm 0.4$	$9.4 \pm 0.9$	$3\sigma: < 2.2$
...	24, 100, 160	$2.6 \pm 0.3$	$2.7 \pm 0.3$	$2.0 \pm 0.3$	$3.6 \pm 0.4$	$15.5 \pm 0.7$	$3\sigma: < 2.2$
...	24, 100, 160, 1.4	$2.6 \pm 0.4$	$2.6 \pm 0.3$	$2.0 \pm 0.4$	$3.5 \pm 0.5$	$15.0 \pm 0.8$	$3\sigma: < 2.2$
Elbaz+11-SB Lum-Eq Weight <sup>f</sup>	24, 100, 160, 1.4	$2.3 \pm 0.2$	$2.0 \pm 0.1$	$1.7 \pm 0.2$	$2.4 \pm 0.2$	$8.8 \pm 0.2$	$3\sigma: < 2.2$
CE01 Lum <sup>e</sup>	24	$3.4 \pm 0.4$	$2.6 \pm 0.2$	$1.7 \pm 0.2$	$4.1 \pm 0.3$	$13.3 \pm 1.1$	$0.4 \pm 0.1$
...	100	$2.4 \pm 0.3$	$2.3 \pm 0.4$	$1.6 \pm 0.5$	$3.1 \pm 0.6$	$10.9 \pm 1.2$	$3\sigma: < 2.3$
...	160	$2.2 \pm 0.3$	$1.8 \pm 0.4$	$1.5 \pm 0.4$	$2.1 \pm 0.6$	$7.9 \pm 1.2$	$1.2 \pm 0.8$
...	100, 160	$2.3 \pm 0.3$	$2.0 \pm 0.3$	$1.6 \pm 0.3$	$2.7 \pm 0.4$	$9.4 \pm 0.9$	$3\sigma: < 2.3$
...	24, 100, 160	$2.4 \pm 0.3$	$2.3 \pm 0.3$	$1.6 \pm 0.3$	$3.3 \pm 0.4$	$12.3 \pm 0.4$	$3\sigma: < 2.3$
...	24, 100, 160, 1.4	$2.4 \pm 0.4$	$2.3 \pm 0.3$	$1.6 \pm 0.4$	$3.2 \pm 0.4$	$12.1 \pm 0.6$	$3\sigma: < 2.3$
CE01 Lum-Eq Weight <sup>f</sup>	24, 100, 160, 1.4	$2.2 \pm 0.2$	$1.8 \pm 0.1$	$1.5 \pm 0.2$	$2.3 \pm 0.2$	$8.2 \pm 0.2$	$3\sigma: < 2.3$
CE01 Col <sup>g</sup>	100, 160	$2.1 \pm 0.4$	$1.8 \pm 0.5$	$2.1 \pm 1.0$	$1.7 \pm 0.6$	$7.9 \pm 1.5$	...
...	24, 100, 160	$2.3 \pm 0.6$	$2.2 \pm 0.8$	$1.6 \pm 0.9$	$3.0 \pm 1.2$	$10.4 \pm 2.3$	...
CE01 Col-Eq Weight <sup>h</sup>	24, 100, 160, 1.4	$2.4 \pm 0.7$	$2.2 \pm 0.8$	$1.6 \pm 0.9$	$3.0 \pm 1.2$	$12.1 \pm 2.7$	...
DH02 Lum <sup>e</sup>	24	$3.0 \pm 0.4$	$2.3 \pm 0.2$	$1.7 \pm 0.2$	$3.6 \pm 0.3$	$21.5 \pm 0.6$	$0.6 \pm 0.1$
...	100	$2.1 \pm 0.3$	$2.0 \pm 0.4$	$1.5 \pm 0.5$	$2.7 \pm 0.5$	$7.8 \pm 0.9$	$3\sigma: < 2.0$
...	160	$2.2 \pm 0.3$	$1.8 \pm 0.4$	$1.6 \pm 0.4$	$2.1 \pm 0.6$	$7.4 \pm 1.2$	$1.3 \pm 0.9$
...	100, 160	$2.1 \pm 0.2$	$1.9 \pm 0.2$	$1.5 \pm 0.3$	$2.5 \pm 0.4$	$7.7 \pm 0.6$	$3\sigma: < 2.0$
...	24, 100, 160	$2.3 \pm 0.3$	$2.2 \pm 0.2$	$1.6 \pm 0.2$	$3.0 \pm 0.4$	$13.6 \pm 0.7$	$3\sigma: < 2.0$
...	24, 100, 160, 1.4	$2.3 \pm 0.3$	$2.2 \pm 0.3$	$1.6 \pm 0.3$	$3.0 \pm 0.5$	$13.2 \pm 0.8$	$3\sigma: < 2.0$
DH02 Lum-Eq Weight <sup>f</sup>	24, 100, 160, 1.4	$2.2 \pm 0.2$	$1.8 \pm 0.1$	$1.6 \pm 0.2$	$2.2 \pm 0.2$	$7.4 \pm 0.2$	$3\sigma: < 2.0$
DH02 Col <sup>g</sup>	100, 160	$2.2 \pm 0.4$	$1.5 \pm 0.5$	$1.7 \pm 0.7$	$1.7 \pm 0.6$	$6.9 \pm 1.3$	...
...	24, 100, 160	$2.4 \pm 0.7$	$2.1 \pm 0.7$	$1.5 \pm 0.8$	$2.8 \pm 1.1$	$10.5 \pm 2.4$	...
DH02 Col-Eq Weight <sup>h</sup>	24, 100, 160, 1.4	$2.3 \pm 0.6$	$2.2 \pm 0.8$	$1.6 \pm 0.9$	$3.6 \pm 1.5$	$9.5 \pm 2.2$	...
Rieke+09 Lum <sup>e</sup>	24	$5.0 \pm 0.6$	$3.6 \pm 0.3$	$2.0 \pm 0.2$	$6.1 \pm 0.5$	$46.1 \pm 1.3$	$0.5 \pm 0.1$
...	100	$2.5 \pm 0.3$	$2.3 \pm 0.4$	$1.8 \pm 0.6$	$3.0 \pm 0.5$	$8.2 \pm 0.9$	$3\sigma: < 2.3$
...	160	$2.2 \pm 0.3$	$1.9 \pm 0.4$	$1.7 \pm 0.5$	$2.1 \pm 0.6$	$6.1 \pm 0.9$	$1.4 \pm 1.0$
...	100, 160	$2.3 \pm 0.2$	$2.1 \pm 0.2$	$1.7 \pm 0.2$	$2.5 \pm 0.3$	$7.1 \pm 0.6$	$3\sigma: < 2.3$
...	24, 100, 160	$2.3 \pm 0.2$	$2.3 \pm 0.3$	$1.8 \pm 0.3$	$3.1 \pm 0.4$	$11.2 \pm 0.7$	$3\sigma: < 2.3$
...	24, 100, 160, 1.4	$2.3 \pm 0.3$	$2.3 \pm 0.3$	$1.8 \pm 0.4$	$3.0 \pm 0.5$	$11.0 \pm 0.9$	$3\sigma: < 2.3$
Rieke+09 Lum-Eq Weight <sup>f</sup>	24, 100, 160, 1.4	$2.2 \pm 0.2$	$1.9 \pm 0.1$	$1.7 \pm 0.2$	$2.2 \pm 0.2$	$6.3 \pm 0.2$	$3\sigma: < 2.3$
Rieke+09 Col <sup>g</sup>	100, 160	$3.1 \pm 0.6$	$2.8 \pm 0.8$	$2.4 \pm 1.3$	$3.6 \pm 1.3$	$12.5 \pm 2.7$	...
...	24, 100, 160	$2.7 \pm 0.7$	$2.4 \pm 0.8$	$1.8 \pm 1.0$	$3.2 \pm 1.3$	$11.9 \pm 2.7$	...
Rieke+09 Col-Eq Weight <sup>h</sup>	24, 100, 160, 1.4	$2.6 \pm 0.7$	$2.3 \pm 0.8$	$1.8 \pm 0.9$	$3.1 \pm 1.2$	$12.1 \pm 2.7$	...

Radio-IR correlation;  
Elbaz+11 templates,  
CE+01, DH+02,  
Rieke+09

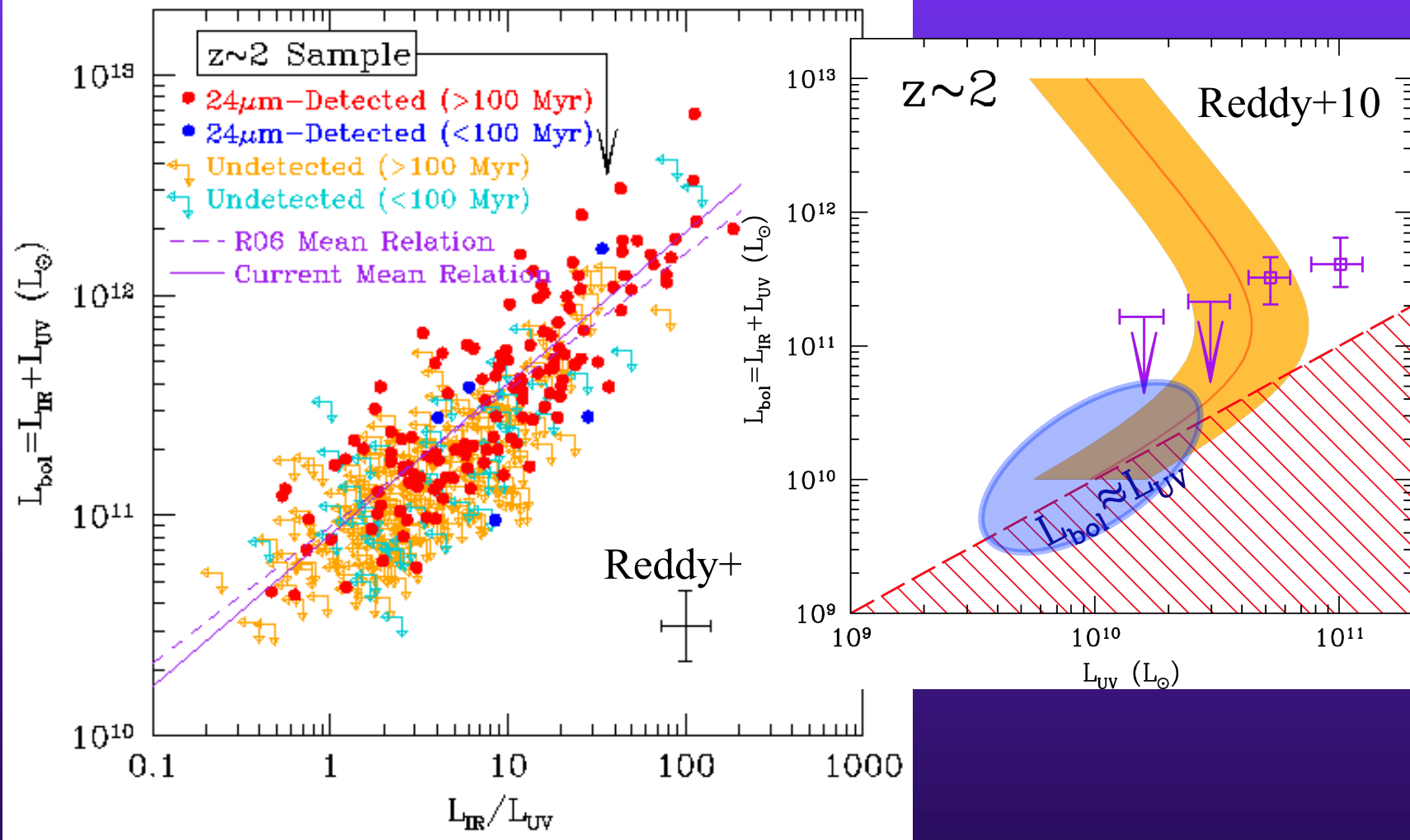
+

Different  
combinations of  
Spitzer / Herschel /  
VLA data

$L_{\text{IR}}$  similar

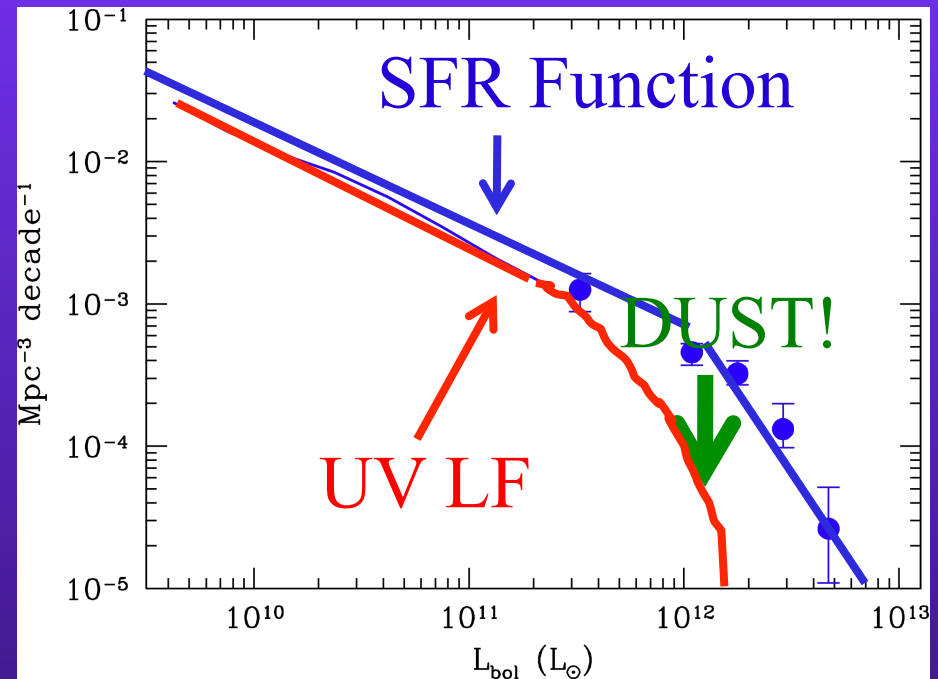
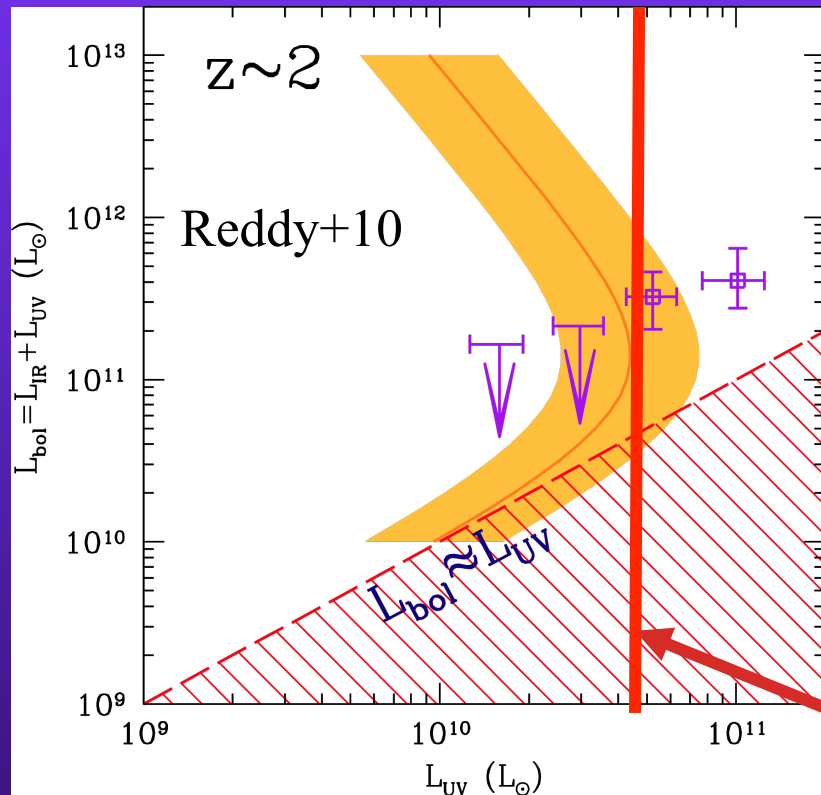


# UV Faint Galaxies Are Less Bolometrically Luminous on Average...





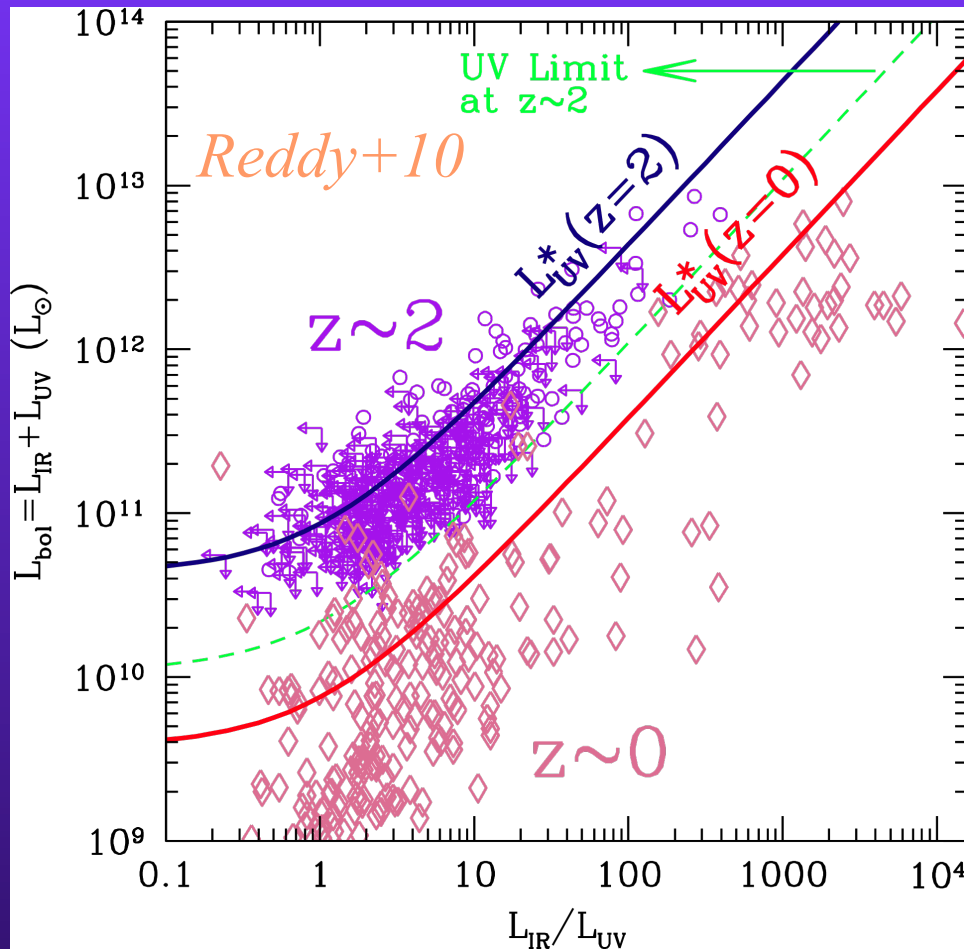
# Effect of Dust on the Galaxy Luminosity Function



Saturation of UV  
luminosity around  
 $L^*(\text{UV})$

Dust affects UV LF and therefore our interpretation of how it evolves with redshift

# Redshift Evolution of Dust Extinction

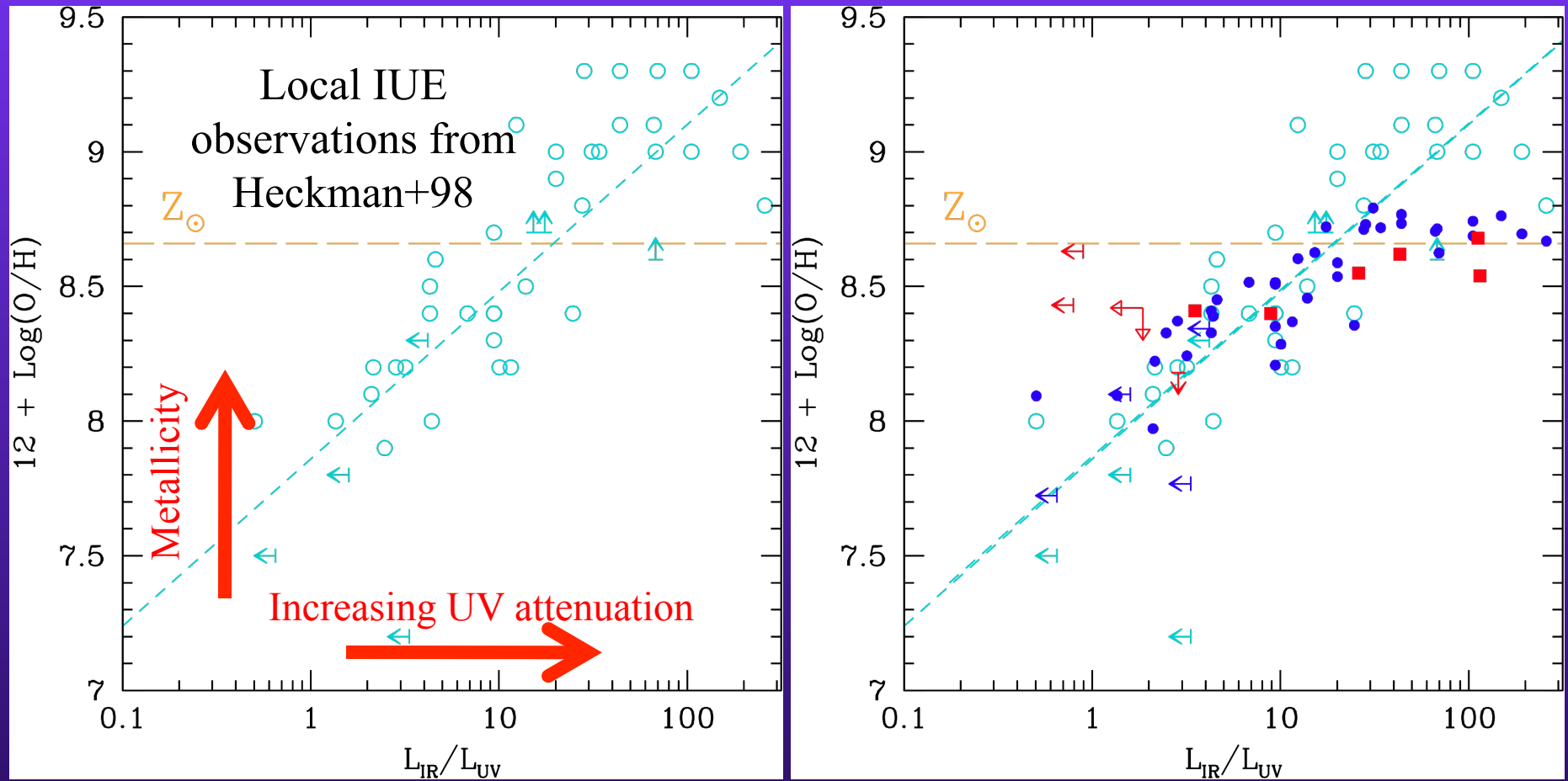


- Tight relation between  $L(\text{bol})$  and dust
- At fixed  $L(\text{bol})$ ,  $z \sim 2$  galaxies less dusty than  $z \sim 0$  galaxies
- Evolution in extinction per unit SFR due to increasing dust-to-gas ratio?

*Reddy+10, Buat+08, Burgarella +08, Daddi+07, Zoran+06, Adelberger & Steidel 2000, Reddy +06, Wang & Heckman 96,*

$Z \gg 2$  UV Dropout selections are likely to be more complete for high SFR galaxies (if they exist) than inferred from local observations

# Physical Mechanism behind L(bol) vs. Dustiness Relation



Evolution of L(bol) vs. Dustiness relation  
directly tied to metallicity evolution

# Conclusions

**FOCUS:** bring multi-wavelength information we have for high redshift galaxies into a coherent picture for the evolution of dust with galaxy luminosity and redshift:

- $L^*$  galaxies at  $z \sim 2$  are LIRGs ( $\sim 2e10 L_{\text{sun}}$ )
- Dust attenuation of UV-bright galaxies  $\sim 4-5$ , similar to prediction from the UV slope
- Dust limits the maximum UV luminosity of star-forming galaxies, thus affecting the shape of the UV luminosity function
- Evolution of extinction per unit star formation rate, likely tied to a change in metallicity as galaxies age